FEBS Letters

FEBS PRESS science publishing by scientists

Cytosolic localization of NADH cytochrome b_5 oxidoreductase (Ncb5or)

Veronika Zámbó[1], Mónika Tóth[1], Krisztina Schlachter[2], Péter Szelényi[1], Farkas Sarnyai[1], Gábor Lotz[2], Miklós Csala[1] and Éva Kereszturi[1]

1 Department of Medical Chemistry, Molecular Biology and Pathobiochemistry, Semmelweis University, Budapest, Hungary
2 2nd Department of Pathology, Semmelweis University, Budapest, Hungary

Correspondence
M. Csala, Department of Medical Chemistry, Molecular Biology and Pathobiochemistry, Semmelweis University, PO Box 2, H-1428 Budapest, Hungary
Fax: +36 1 266 26 15
Tel: +36 1 266 26 15
E-mail: csala.miklos@med.semmelweis-univ.hu

(Received 19 December 2015, revised 29 January 2016, accepted 4 February 2016, available online 26 February 2016)

doi:10.1002/1873-3468.12097

Edited by Peter Brzezinski

Acyl-CoA desaturation in the endoplasmic reticulum (ER) membrane depends on cytosolic NADH or NADPH, whereas NADPH in the ER lumen is utilized by prereceptor glucocorticoid production. It was assumed that NADH cytochrome b_5 oxidoreductase (Ncb5or) might connect Acyl-CoA desaturation to ER luminal redox. We aimed to clarify the ambiguous compartmentalization of Ncb5or and test the possible effect of stearoyl-CoA on microsomal NADPH level. Amino acid sequence analysis, fluorescence microscopy of GFP-tagged protein, immunocytochemistry, and western blot analysis of subcellular fractions unequivocally demonstrated that Ncb5or, either endogenous or exogenous, is localized in the cytoplasm and not in the ER lumen in cultured cells and liver tissue. Moreover, the involvement of ER-luminal reducing equivalents in stearoyl-CoA desaturation was excluded.

Keywords: endoplasmic reticulum; fatty acid desaturation; glucocorticoid; pyridine nucleotides; redox state

Fatty acid synthesis yields saturated chains, dominantly of 16 carbon atoms in human cells. Palmitoic acid (C16 : 0) serves as the common endogenous precursor for various other nonessential fatty acids. Its processing starts with an ATP-dependent activation, that is, the formation of palmitoyl-CoA, and the intermediates remain bound to the carrier molecule [1]. The chain can be modified through variable sequences of elongation (addition of two carbons) and desaturation (changing a single into a double bond) [2]. Exogenous essential or nonessential fatty acids are also attached to CoA, and they can undergo the same intracellular modifications to maintain a balanced fatty acyl-CoA supply for the synthesis of complex lipids. The fatty acyl-CoA elongase and desaturase enzyme systems are embedded in the endoplasmic reticulum (ER) membrane [2], and these transformations do not require the acyl-CoA intermediates to cross the membrane and enter the ER lumen [3].

Acyl-CoA desaturation means elimination of two electrons (H atoms) from two neighboring carbon atoms of the saturated chain. This oxidation is carried out indirectly, through inserting an oxygen atom and subsequently removing a water molecule. The remaining oxygen atom of the substrate oxygen molecule needs to be reduced, and hence the overall process consumes the cell's reducing power. Similarly to other mono-oxygenases in the ER membrane (i.e., cytochrome P450s), fatty acyl-CoA desaturases of human and animal cells function as terminal members of electron transfer chains, which deliver two electrons from NADH or NADPH to molecular oxygen [4].

Abbreviations
DAPI, 4′,6-diamidin-2-phenylindol; DIC, differential interference contrast; DMEM, Dulbecco's modified Eagle's medium; ER, endoplasmic reticulum; FBS, fetal bovine serum; GAPDH, glyceraldehyde-3-phosphate dehydrogenase; H6PD, hexose 6-phosphate dehydrogenase; HEPES, 4-(2-hydroxyethyl)piperazine-1-ethanesulfonic acid; Ncb5or, NADH cytochrome b_5 oxidoreductase; RT, room temperature.

The first double bond is formed at carbon 9 in the saturated acyl-CoAs (palmitoyl- or rather stearoyl-CoAs) by Stearoyl-CoA desaturase (SCD) (EC 1.14.99.5) [5]. Humans have two SCD homologues (SCD1 and SCD5). The former is ubiquitous in the organism and it is highly expressed in the liver and adipose tissue, while the latter is mostly expressed in the brain and pancreas [6]. The electron transfer chain that connects NAD(P)H and the nonheme iron in the active site of SCD1 comprises the flavoprotein cytochrome b_5 reductase (*b*5R) and the hemoprotein cytochrome b_5 (*b*5). These two monomeric dehydrogenase enzymes are post-translationally targeted and get tail-anchored into the ER membrane [7]. The amino-terminal bulk of their polypeptide chains, that is, the FAD-containing catalytic domain of *b*5R [8] and the heme-containing catalytic portion of *b*5 [9] are located at the cytosolic side of the lipid bilayer. In accordance with this membrane topology, it has been demonstrated that acyl-CoA desaturation is driven by the cytosolic rather than the ER luminal NAD(P)H pool [10–12].

The recent discovery of NADH cytochrome b_5 oxidoreductase (Ncb5or; EC 1.6.2.2) has raised the possibility that this novel enzyme might serve as an alternative electron supplier for SCD1. Ncb5or is a soluble natural fusion protein that integrates both *b*5R-like and *b*5-like domains with FAD and heme prosthetic groups, respectively. Cooperation of these two domains can transfer electrons from NAD(P)H to various artificial substrates [13]. Although the physiological substrate(s) and the exact function of Ncb5or remain to be elucidated, the domain structure of the enzyme strongly suggests its role in fatty acid desaturation. This theory is further supported by the phenotype of Ncb5or knock-out mice, which includes a progressive loss of white adipose tissue along with a pronounced reduction in the ratios of Δ^9 desaturated to saturated fatty acids in the liver [14].

Since the first report on the ER localization of Ncb5or [15], the enzyme is generally referred to as a microsomal oxidoreductase in accordance with its putative function. Microsomal localization of the particulate, that is, nonmembrane-bound Ncb5or protein implies either its attachment to integral membrane proteins on the cytosolic surface of the ER or its luminal emplacement within the organelle. The former option would only provide an alternative means of draining the cytosolic reducing power toward SCD1; however, the latter topology raises the intriguing possibility that ER luminal NADPH may be utilized in the process of acyl-CoA desaturation. The ER luminal $NADP^+$:NADPH redox state is a major determinant of prereceptor glucocorticoid production [16], that is, the concerted activity of NADPH-dependent type 1 11β-hydroxysteroid dehydrogenase (11βHSD1) and $NADP^+$-dependent hexose 6-phosphate dehydrogenase (H6PD) [17]. Draining microsomal NADPH to acyl-CoA desaturation would, therefore, create a direct link between cellular lipid metabolism and local modulation of glucocorticoid hormone action in the target cells.

It is essential to identify the subcellular compartment that homes Ncb5or, and particularly to clarify whether Ncb5or can access the separate NADPH pool of the ER. The present work addressed these questions by investigating the intracellular localization of overexpressed or endogenous Ncb5or in cultured cells and in the liver tissue using fluorescent microscopy and cell fractioning. The putative effect of stearoyl-CoA administration on luminal [NADPH]:[$NADP^+$] ratio in liver microsomes has been also tested. Our results unequivocally demonstrate that the novel oxidoreductase is a cytosolic enzyme, which has no access to the luminal ER redox environment.

Materials and methods

Materials used

Lipofectamine 2000 and BODIPY™ TR-X thapsigargin were purchased from Invitrogen. pcDNA3.1- and pEGFP-N1 plasmids were from Clontech Laboratories, Inc. (Mountain View, CA). Dulbecco's modified Eagle's medium (DMEM), Opti-MEM, fetal bovine serum (FBS), 1% antibiotic–antimycotic solution and trypsin-EDTA (0.25%) were obtained from Thermo Fisher Scientific (Waltham, MA). Cortisone, metyrapone, stearoyl-CoA, G6P, 4-morpholinepropanesulfonic acid (MOPS) and 4-(2-Hydroxyethyl)piperazine-1-ethanesulfonic acid (HEPES) were purchased from Sigma Chemical, St. Lous, MO.

Prediction of subcellular localization

The following computational tools were used to predict subcellular targeting and localization of Ncb5or: BACELLO (http://gpcr.biocomp.unibo.it/bacello), CELLO v.2.5 (http://cello.life.nctu.edu.tw/), ESLDB (http://gpcr.biocomp.unibo.it/esldb/), EUK-MPLOC 2.0 (http://www.csbio.sjtu.edu.cn/bioinf/euk-multi-2), PROTEINPROWLER (http://bioinf.scmb.uq.edu.au:8080/pprowler_webapp_1-2), and YLOC (http://abi.inf.uni-tuebingen.de/Services/YLoc/webloc.cgi).

Expression plasmid constructions

The coding sequence of human NCB5OR was PCR amplified by using NCB5OR-XhoI sense (5′-AAA TTT CTC GAG GGG TTT GAA GAT GCT GAA C-3′) and NCB5OR-HindIII antisense (5′-AAA TTT AAG CTT

GTT GAA TAA AGG ACA ATG ACA G-3′) primers. The template cDNA had been produced by reverse transcription of mRNA isolated from HepG2 cells. The purified PCR product was cloned into pcDNA3.1- and pEGFP-N1 plasmids between their XhoI and HindIII restriction sites. All constructs were verified by sequencing.

Cell cultures, transient transfection and lysis

Human embryonic kidney (HEK) 293T cells and hepatocellular carcinoma (HepG2) cells were cultured in Dulbecco's modified Eagle medium (DMEM) supplemented with 10% fetal bovine serum and 1% penicillin/streptomycin solution at 37 °C in a humidified atmosphere containing 5% CO_2.

For transient transfection, 6×10^5 HEK293T cells were seeded per well in 6-well plates. Transfection with pcDNA3.1-_NCB5OR, pEGFP-N1_NCB5OR, or empty pEGFP-N1 plasmid (2 μg each) was performed using Lipofectamine 2000 and Opti-MEM according to the manufacturer's instructions. Transfected and parallelly cultured nontransfected (control) cells were processed 48 h after transfection.

Cell lysates were made for western blot analysis by removing the medium, washing the wells with PBS twice and then scraping and briefly vortexing the cells in 100 μL reporter lysis buffer (Promega, Madison, WI, USA). After 15 min incubation at room temperature, the lysates were centrifuged for 5 min at max speed in a benchtop centrifuge at 4 °C to remove cell debris. Protein concentration of the supernatants was measured using Pierce® BCA Protein Assay Kit (Thermo Scientific, Waltman, MA, USA).

Analysis of Ncb5or-EGFP fusion protein

Expression of fluorescent Ncb5or-EGFP fusion protein was analyzed in pEGFP-N1_NCB5OR-transfected HEK293T cells. Forty-eight hours after transfection, cells were washed three times with PBS and fixed in 3.7% formaldehyde for 10 min. After washing in PBS, cells were permeabilized with 0.2% Triton X-100 in PBS for 5 min and then washed in PBS again. Nuclei were stained with DAPI (2 $\mu g \cdot mL^{-1}$, 5 min), the cells were rinsed with PBS, and the ER was labeled with BODIPY™ TR-X thapsigargin (1 μM). Images were taken immediately by using a fluorescence microscope (Leica DMI6000 B with DFCU80 camera) before the development of ER stress-related morphological changes. Transfection efficiency, that is, the relative number of EGFP-positive cells was above 80%.

Integrity of Ncb5or-EGFP fusion protein in the cells was verified by SDS/PAGE and autofluorescence detection. Cell lysates were prepared by freeze-thawing, cell debris was removed by centrifuging, and the supernatant was prepared without DTT and heat denaturation for separation in SDS/PAGE. Fluorescence was detected and gel images were produced by scanning in Typhoon 9400 variable mode imager (Amersham Biosciences, Freiburg, Germany) at 488-nm excitation and 509-nm emission wavelengths.

Separation of subcellular fractions by differential centrifugation

The presence of endogenous Ncb5or was tested in various subcellular (i.e., nuclear, mitochondrial, microsomal, and cytosolic) fractions prepared from nontransfected HEK293 and HepG2 cells as well as from rat livers. HEK293 and HepG2 cells were washed twice, scraped in 1 mL PBS and disrupted by using a Dounce homogenizer. Livers of overnight fasted male Wistar rats (200–250 g body weight) were removed immediately after decapitation of the animals, and they were homogenized in sucrose-HEPES buffer (0.3 M sucrose, 0.02 M HEPES, pH 7.2) buffer by Potter-Elvehjem homogenizer. Cell/tissue debris was sedimented from the homogenates (800 ***g***, 2 min, 4 °C), and the supernatant was subjected to repeated centrifugations of increasing force. The pellet was removed each time and yielded the fractions of nuclei (1000 ***g***, 10 min, 4 °C), mitochondria (11 000 ***g***, 20 min, 4 °C) and microsomes (100 000 ***g***, 1 h, 4 °C), while the cytosolic fraction was gained as the remaining supernatant. Aliquots of each fraction (100 μL) were precipitated with 10% TCA, and the pellets were dissolved in 20 μL sample buffer for western blot analysis. Rat liver microsomes were resuspended in MOPS-KCl buffer (100 mM KCl, 20 mM NaCl, 1 mM $MgCl_2$, and 20 mM MOPS, pH 7.2), rapidly frozen and stored in liquid N_2 until used. Protein concentration of the microsomes was determined with Bio-Rad protein assay solution using bovine serum albumin as a standard according to the manufacturer's instructions.

The origin and purity of each subcellular fraction was confirmed by immunoblot using primary antibodies specific to organelle-specific marker proteins (nucleus: CREB-1 and Lamin A/C; mitochondria: Bcl-X_L and Cyclophilin D; cytoplasm: procaspase-3 and GAPDH; ER: PDI).

Western blot analysis

Cell lysates (50 μg protein) and samples of subcellular fractions were electrophoresed in 12% Tris-glycine minigels and transferred onto Immobilon-P membranes (Millipore, Billerica, MA). The membranes were blocked with 5% nonfat milk powder in phosphate-buffered saline in 0.1% Tween-20 (PBST) solution for 1 h. Primary antibodies were applied overnight at 4 °C, and secondary antibodies for 1 h at room temperature. Primary antibodies and their dilutions: anti-CREB1 (Santa Cruz, sc271), 1 : 2000; anti-Lamin A/C (Cell Signaling, 4777), 1 : 1000; anti-Bcl-X_L (Santa Cruz, sc8392), 1 : 1000; anti-Cyclophilin D (MitoSciences, MSA04), 1 : 1000; anti-PDI (Santa Cruz, sc20132), 1 : 4000; anti-procaspase-3 (Santa Cruz, sc7272), 1 : 4000;

anti-Ncb5or (Santa Cruz, sc-100529 and sc-68684), 1 : 2000, anti-GAPDH (Santa Cruz, 6C5), 1 : 20 000; anti-SCD1 (Abcam, ab19862), 1 : 4000. HRP-conjugated goat anti-(rabbit IgG), horse- anti-(mouse IgG), and donkey anti-(goat IgG) antibodies were purchased from Cell Signaling (7074S; 7076S) and Santa Cruz Biotechnology (sc-2020). They were applied at 1 : 2000 dilution. HRP was detected using SuperSignal West Pico Chemiluminescent Substrate (Pierce).

Immunofluorescence staining and fluorescent microscopy in HepG2 cells

The HepG2 cells were grown on microscope slides in humidity chamber for 6 h. The cells were then fixed in methanol-acetone (1 : 1) for 10 min at room temperature (RT), washed three times 5-min in PBS, permeabilized and blocked in DAKO serum-free protein blocking solution (code: X0909; DAKO, Glostrup, Denmark) for 1 h at RT. Cells were then incubated with the appropriate primary antibodies overnight at 4 °C, followed by staining with fluorochrome-labeled secondary antibodies for 1 h. Primary antibodies were mouse monoclonal antibody against human Ncb5or (1 : 200 dilution; Santa Cruz Biotechnology; sc-100529) and rabbit polyclonal antibody against PDI (1 : 100 dilution; Santa Cruz Biotechnology; sc-20132). Alexa Fluor 488 donkey anti-(mouse IgG) and Alexa Fluor 568 goat anti-(rabbit IgG) (Life Technologies, Walthman, MA, USA) fluorescent secondary antibodies were used (both diluted 1 : 200). Coverslips were mounted on glass slides with 4′,6-diamidin-2-phenylindol (DAPI) containing Vecteshield mounting medium from Vector Laboratories (Burlingame, CA). Fluorescent microscopy was performed using a Leica DM RXA motorized fluorescent microscope (Leica Microsystems GmbH, Wetzlar, Germany) equipped with Spectrum Orange, Spectrum Green, single bandpass, and DAPI single longpass filters, as well as DAPI/FITC/Texas Red triple bandpass filter. Nomarski differential interference contrast (DIC) technique was used to visualize the cells and their borders for the precise localization results. Images were taken at 630-fold magnification by a Leica DFC 365FX high performance monochrome CCD camera controlled by Leica CW4000 FISH software (Leica Microsystems Imaging Solutions Ltd., Cambridge, UK).

Fluorimetric detection of microsomal NADH and NADPH

Endogenous reduced pyridine nucleotide content of intact rat liver microsomes was monitored at 1 $mg{\cdot}mL^{-1}$ protein concentration in MOPS-KCl buffer at 37 °C by fluorimetry. NAD(P)H-specific fluorescence was detected at 340-nm excitation and 460-nm emission wavelengths using a Cary Eclipse spectrofluorimeter (Varian, Woburn, MA). Oxidation of the luminal pyridine nucleotide pool was induced by metyrapone (5 μM) or cortisone (10 μM) and this effect was reverted by G6P (100 μM). Stearoyl-CoA was administered at various concentrations below 100 μM.

Results

In silico prediction of subcellular localization

Elucidated amino acid sequence of human Ncb5or [NCBI: NP_057314.2] was analyzed by computational tools to identify any ER-targeting signals and to predict the subcellular localization of the protein. The results obtained from six online localization predictors are summarized in Table 1. These tools employ various well-documented methods including homology-based annotations, analysis of whole sequence amino acid composition, search for sorting signals and functional motifs. None of the applied tools revealed signal peptide or ER-retention signal in the polypeptide. Although the possibility of mitochondrial or nuclear localization was also speculated as second or third options, the most likely topology of Ncb5or protein was unequivocally predicted to be cytoplasmic (Table 1).

Expression and fluorescent detection of Ncb5or-EGFP fusion protein in HEK293T cells

The HEK293T cells were transiently transfected with pcDNA3.1-_NCB5OR, pEGFP-N1_NCB5OR, or empty pEGFP-N1 plasmid constructs to express exogenous human Ncb5or, Ncb5or-EGFP fusion protein, or EGFP, respectively. Prior to fluorescence microscopy, the expression, stability and intactness of Ncb5or-EGFP was tested using gel electrophoresis and autofluorescence detection as well as immunoblot with anti-Ncb5or primary antibody. Fluorescent signals of EGFP (27 kDa) and Ncb5or-EGFP (86 kDa) were clearly visible at the appropriate molecular weights in polyacrylamide gels after separation (Fig. 1A). Most importantly, the 27 kDa band corresponding to EGFP alone was not detectable in the samples prepared from Ncb5or-EGFP-expressing cells, which indicates the lack of significant intracellular breakage of the tagged protein. A small amount of endogenous Ncb5or was revealed in the protein lysates of control (untransfected) cells by western blot analysis. As it was expected, the overexpression of untagged Ncb5or was demonstrated by a largely intensified band of the same molecular weight (59 kDa) in pcDNA3.1-_NCB5OR-transfected cells (Fig. 1B). The applied anti-Ncb5or primary antibody yielded two bands in the samples of pEGFP-N1_NCB5OR-transfected cells: the stronger

Table 1. Prediction of subcellular localization of human Ncb5or

Software	Localization	Basis of prediction
eSLDB	Cytoplasm	Homology-based annotations (28)
CELLO v.2.5	Cytoplasm RELIABILITY: Cytoplasmic 1.969 Nuclear 1.510 Mitochondrial 1.092 Peroxisomal 0.049 PlasmaMembrane 0.048 ER 0.032	Amino acid composition, the partitioned amino acid composition and the sequence composition based on the physico-chemical properties of amino acids (29)
YLoc	Cytoplasm PROBABILITY: Cytoplasm 84.6% Mitochondrion 9.1% Nucleus 6.3% Secretory pathway 0.0%	Sequence-based predictions (amino acid composition, sorting signals) (30)
BaCelLo	Cytoplasm LOCALIZATION STEPS: Intracellular → Nucleus or Cytoplasm → Cytoplasm	Amino acid compositions of both the N- and C-terminal (31)
Euk-mPLoc 2.0	Cytoplasm	Gene ontology, functional domains and sequential evolutionary information (32)
ProteinProwler	Cytoplasm	N-terminal sequence motifs (33)

The entire amino acid sequence of human Ncb5or [NCBI: NP_057314.2] was analyzed by six online computational softwares employing different algorithms (see references) to predict the subcellular localization of the protein. Further details of the output are shown where available.

one indicates EGFP-tagged protein of 86 kDa, while the fainter one can be identified as the 59 kDa Ncb5or without EGFP-tag. The latter did not significantly exceed the endogenous expression seen in the control samples, which further supports the stability of Ncb5or-EGFP polypeptide (Fig. 1B).

After having verified that pEGFP-N1_NCB5OR-transfected cells are free of interfering protein degradation products, and EGFP-specific fluorescence corresponds to Ncb5or-EGFP, these cells were examined by flurescence microscopy. Green autofluorescence was observed in more than 80 of 100 investigated cells, that is, the transfection efficiency was above 80%. The signal was diffuse in the cytoplasm (Fig. 2), and it did not colocalize with fluorescent staining of either the nuclei (DAPI, blue) or the ER (BODIPY™ TR-X thapsigargin, red).

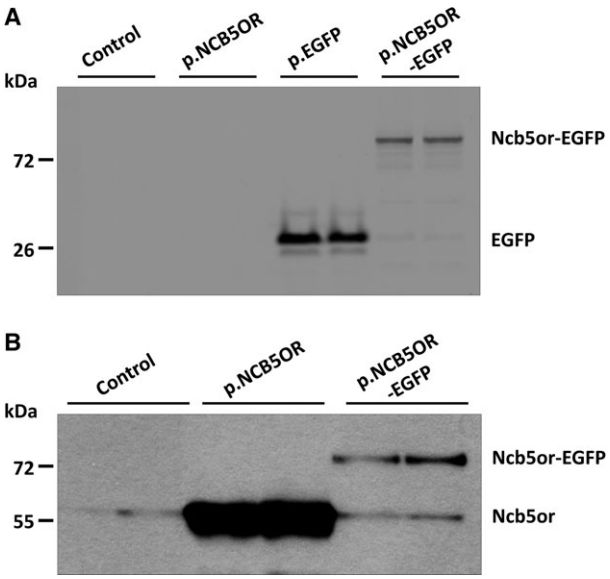

Fig. 1. Expression and integrity of Ncb5or-EGFP fusion protein. Control (nontransfected) and transfected (p.NCB5OR, p.EGFP, or p.NCB5OR-EGFP) HEK293T cells were harvested and lysed 48 h after transfection. Equal amounts of proteins (50 μg) were electrophoresed in a 12% SDS-polyacrylamide gel, and (A) their green fluorescence was scanned by a gel imager at 488-nm excitation and 509-nm emission wavelengths, or (B) they were transferred to Immobilon-P membrane and visualized by western blot using an anti-Ncb5or antibody. The calculated weights of Ncb5or-EGFP fusion protein, Ncb5or and EGFP, are 86 kDa, 59 kDa and 27 kDa, respectively. Typical results of three independent experiments are shown.

Ncb5or immunoblot in isolated subcellular fractions

Intracellular localization of Ncb5or was further analyzed by detecting the endogenously expressed protein in subcellular fractions prepared by differential centrifugation from HEK293 and HepG2 cells as well as from rat livers. Proteins of well-defined localization and regarded as characteristic to different cellular compartments or organelles were employed as markers specific to each fraction in our experiments. The markers of nuclei (CREB-1 and Lamin A/C), ER (PDI) and cytosol (Procaspase-3 and GAPDH) were detected only in the appropriate samples, while some contamination of nuclear fractions with mitochondria was indicated by the presence of mitochondrial markers (Bcl-X_L or Cyclophilin D) in both lanes, mostly in HEK293 and rat liver samples (Fig. 3). This, however, did not disturb the evaluation of our assay as Ncb5or protein could be detected only in the cytosolic fractions of both of the cultured cells and of rat livers.

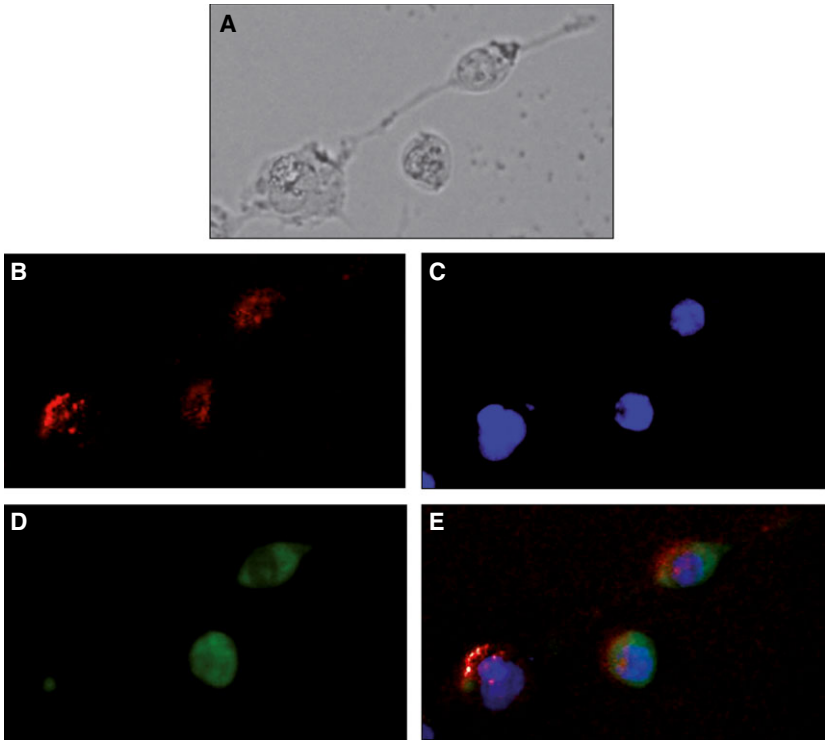

Fig. 2. *In situ* localization of Ncb5or-EGFP fusion protein in HEK293T cells. (A) HEK293T cells were transfected with p.NCB5OR-EGFP construct and studied by fluorescence microscopy 48 h after transfection. (B) Endoplasmic reticulum was labeled with BODIPY™ TR-X (red). (C) Nuclei were stained with DAPI (blue). (D) Green fluorescence of Ncb5or-EGFP fusion protein was detected in more than 80 of 100 cells (above 80% transfection efficiency). (E) merged image of B, C, and D. Typical results of four independent experiments are shown.

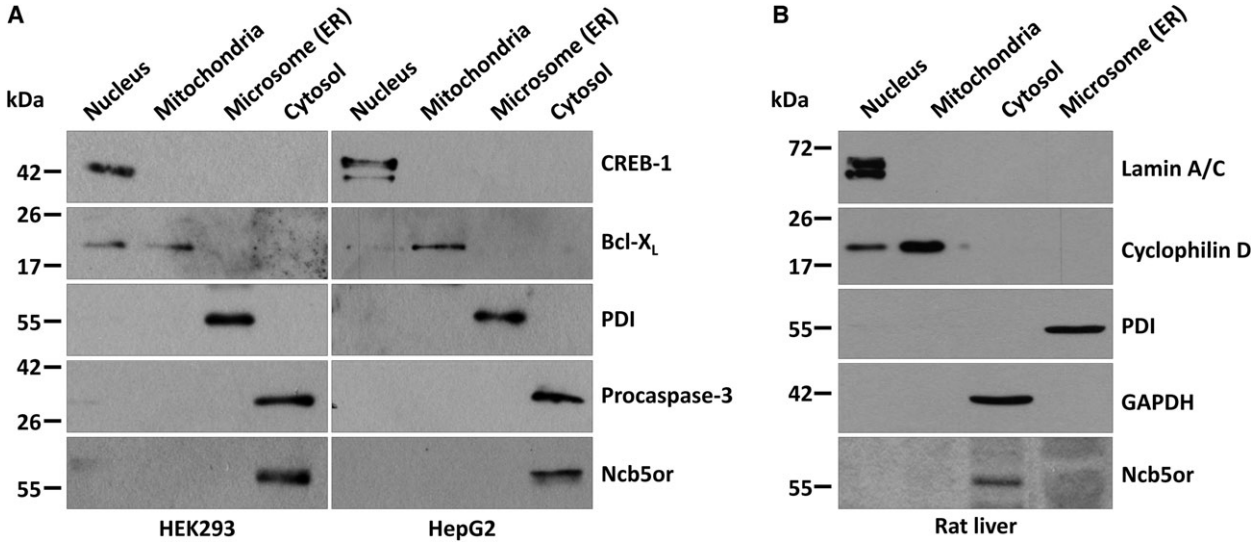

Fig. 3. Detection of endogenous Ncb5or protein in different subcellular fractions. HEK293 and HepG2 cells (A) and rat liver tissue (B) were homogenized and their subcellular fractions were separated by differential centrifugation. Aliquots of each fraction were subjected to SDS/PAGE, transferred to Immobilon-P membrane and analyzed by immunoblot. CREB1 (cAMP-responsive element-binding protein 1) and Lamin A/C nuclear, Bcl-X_L (B-cell lymphoma-extra large) and Cyclophilin D mitochondrial, PDI (Protein disulfide isomerase) microsomal, procaspase-3 and glyceraldehyde-3-phosphate dehydrogenase (GAPDH) cytosolic markers as well as Ncb5or were detected by using specific primary antibodies. Typical results of four independent experiments are shown.

Immunocytochemistry of endogenous Ncb5or in HepG2 cells

To avoid the drawbacks of exogenous overexpression and peptide tagging that might affect intracellular protein targeting, while taking advantage of *in situ* analysis, endogenously expressed naive Ncb5or was immunolabeled and localized by fluorescence microscopy in untreated and untransfected HepG2 cells (Fig. 4).

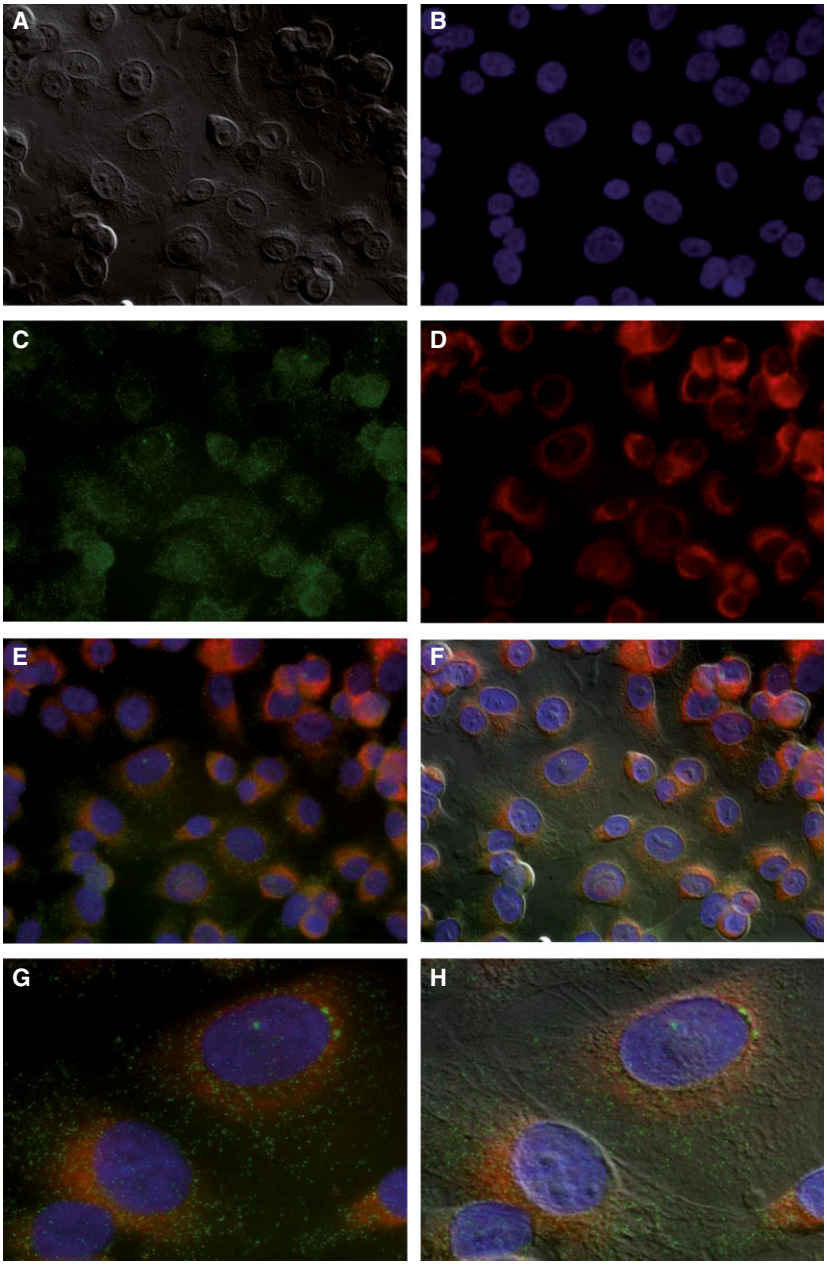

Fig. 4. Immunocytochemistry of endogenous Ncb5or protein in HepG2 cells. Immunofluorescence shows the subcellular localization of Ncb5or protein (green) and the endoplasmic reticulum (ER) marker protein disulfide isomerase (PDI, red) in HepG2 cells (original magnification: 630×). (A) Differential interference contrast (DIC) image of HepG2 cells. (B) The nuclei were stained with DAPI. (C) Localization of Ncb5or protein visualized by specific primary antibody and Alexa 488-conjugated (green fluorescent) secondary antibody. (D) Endoplasmic reticulum was stained with a specific antibody against PDI followed by a secondary antibody labeled with Alexa 568 fluorescent red dye. (E, G) Merged images of B, C, and D. (F, H) Merged DIC images of B, C, and D. Typical results of three independent experiments are shown.

The specific (green) signal for Ncb5or was seen to be disseminated in the cytosol, showing a clearly different pattern compared to the ER labeling (red). The Nomarski DIC technique is capable to visualize cells and their borders by transforming the invisible optical density differences into visible, relief-like picture of the object. Endogenous expression of Ncb5or was demonstrated to be quite low by immunocytochemistry. However specificity of this weak staining was supported by the fact that the small green dots corresponding the Ncb5or-specific signals were definitely localized within the Nomarski DIC visualized cell borders. In certain cells, Ncb5or seemed to be localized in the processes of the cytoplasm as well, while others lacked the Ncb5or protein in their cytoplasmic extensions. Accumulation of Ncb5or at the nuclear border was also observed in a few cells. Nevertheless, the protein did not show obvious colocalization with either the nuclear staining or the ER labeling.

Effect of stearoyl-CoA on the microsomal pyridine nucleotides

Although the above data did not support the assumption that Ncb5or might create a link between

ER-luminal pyridine nucleotides and acyl-CoA desaturation in the membrane, the possible effect of stearoyl-CoA on the luminal redox state was checked in rat liver microsomal vesicles. Ncb5or is assumed to substitute for both *b*5 and *b*5R in the electron flow. The presence of SCD1 in the microsome preparation was first confirmed by western blot analysis using anti-SCD1 antibody and a lysate of SCD1-transfected HEK293T cells for positive control (Fig. 5D). The well-established method based on continuous fluorimetric monitoring of intrinsic luminal NADH and NADPH is suitable to reveal redox shifting inside the vesicles (Fig. 5). Oxidation was clearly detected upon the addition of metyrapone or cortisone (substrates of 11βHSD1) and their effect could be antagonized by glucose-6-phosphate (a substrate of H6PD). However, fluorescence was not altered by repeated addition of stearoyl-CoA, that is, the luminal NAD(P)H level remained unaffected by the substrate of microsomal stearoyl-CoA desaturase (Fig. 5).

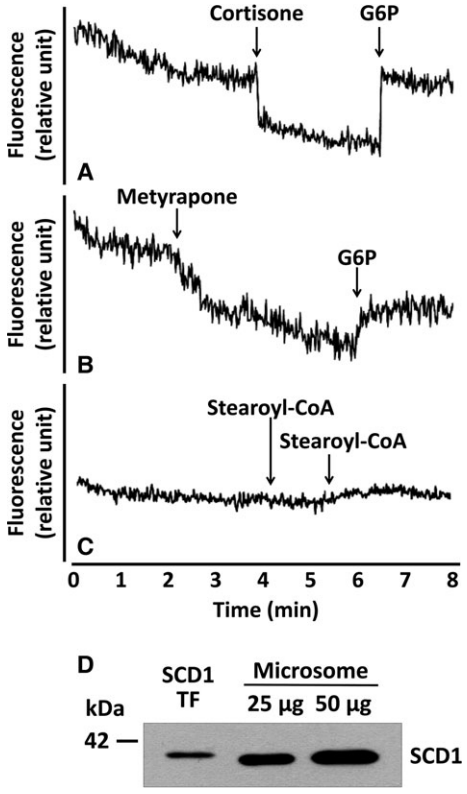

Fig. 5. Modulation of NADPH level in the microsomal lumen. Endogenous NADPH content of intact rat liver microsomal vesicles was monitored at 1 mg·mL^{-1} protein concentration in MOPS-KCl buffer by detecting fluorescence at 340 nm excitation and 460 nm emission wavelengths. A decrease in the fluorescence signal corresponds to the oxidation of luminal pyridine nucleotides. Cortisone (A) and metyrapone (B) were added at 10 µM final concentration and followed by 100 µM glucose 6-phosphate (A and B) as indicated by the arrows. Stearoyl-CoA (C) was administered repeatedly (first at 10 µM and then at 50 µM concentration). (D) Western blot analysis of the microsome preparation using anti-SCD1 antibody and a lysate of SCD1-transfected HEK293T cells (SCD1 TF) for positive control. Typical results of three independent experiments are shown.

Discussion

Controversial data have been published regarding the subcellular topology of Ncb5or. The first report on the newly discovered protein demonstrated its cytosolic perinuclear localization [18]. These findings were revised 5 years later, and Ncb5or was shown to be localized in the ER by using immunocytochemistry on COS-7 cells expressing exogenous human truncated c-myc-tagged Ncb5or, which was also supported by the enzyme's colocalization with calreticulin [15]. The question has not been addressed again, and Ncb5or is now generally considered as a microsomal enzyme, which implies its ER luminal emplacement considering the lack of transmembrane domains and membrane-anchoring moieties in the single polypeptide.

Particulate microsomal proteins usually contain two targeting signals, an amino-terminal or internal signal peptide [19] and a carboxyl-terminal ER retention signal [20]. The lack of established ER retention signals in the polypeptide chain does not on its own rule out the localization in the lumen of the organelle. For instance, the ER location of microsomal glucuronidase, void of any intrinsic ER retention sequence, is a secondary result of association with egasyn, which is retained within the lumen of the ER [21] via an HTEL ER retention sequence [22]. However, the signal peptide is considered as a structural feature both necessary and sufficient for ER-targeting [19]. It is not surprising, therefore, that *in silico* peptide analysis using various tools unequivocally predict against ER-targeting of Ncb5or as it possesses neither signal peptide nor retention sequence.

Although the physiologically interacting protein partners of Ncb5or have not been identified, the presence of both *b*5R-like and *b*5-like domains in the polypeptide and the data obtained from *in vitro* activity measurements suggest the involvement of the enzyme in fatty acyl-CoA desaturation as an alternative electron supplier. This hypothesis is further supported by the phenotype of Ncb5or$^{-/-}$ mice showing a characteristic alteration of saturated-unsaturated fatty acid profile. Since the reactions of acyl-CoA desaturation take place at the interface of two cellular compartments of separate pyridine nucleotide pools, it

is a highly relevant question whether the acyl-CoA desaturation is driven by cytosolic or ER luminal NAD(P)H. The ER membrane is not permeable to pyridine nucleotides (i.e., NAD^+, NADH, $NADP^+$, and NADPH). Therefore, the ER luminal $NAD(P)^+$-NAD(P)H redox cycles are largely independent of the cytosolic redox conditions [23]. The best known and quantitatively by far the most important NADPH consuming reaction is the reduction of cortisone to cortisol by 11βHSD1 in the ER lumen of most tissues (e.g., liver, muscle, adipose tissue). This in turn is fueled by local NADPH production, which is maintained by the luminal $NADP^+$-dependent H6PD [17]. The concerted action of these two coupled enzymes is responsible for the prereceptor cortisol generation, and hence it largely affects the local glucocorticoid action in most hormone-targeted tissues. It has been demonstrated that modulations in the redox state of ER luminal pyridine nucleotides contribute to nutrient sensing by the organelle [16]. Moreover, mounting evidence support the role of microsomal prereceptor cortisol production in the metabolic syndrome [24]. Therefore, any relationship between the separate ER luminal pyridine nucleotide redox system and fatty acid desaturation would clearly provide a means by which saturated fatty acids can directly interact with the hormonal control of major cellular functions, and this option would give new perspectives to lipotoxicity research.

The possibility that Ncb5or might link ER luminal redox to acyl-CoA desaturation was suggested by all available data regarding Ncb5or (i.e., NADH- or NADPH-dependence, interacting domains similar to *b*5R and *b*5, microsomal localization, defective fatty acid desaturation, increased lipotoxicity and diabetes in the knockout animals). Therefore, we aimed to clarify the ambiguous subcellular topology of this soluble protein. We addressed the question by using fluorescence microscopy of GFP-tagged fusion protein, immunocytochemistry and western blot analysis of subcellular fractions prepared from cultured cells or liver tissue. Our results unequivocally demonstrated the cytosolic localization of either exogenous and tagged or endogenous and naive Ncb5or. The possible effect of stearoyl-CoA on the ER luminal pyridine nucleotides was also tested in liver microsomes. The well-established fluorescent method has been repeatedly proven to reveal any redox shifting in the intrinsic $NAD(P)^+$-NAD(P)H pool upon the activity of luminal dehydrogenases [25–27]. Cortisone or metyrapone caused a remarkable oxidation of NAD(P)H, which was reverted by glucose 6-phosphate; however, stearoyl-CoA remained ineffective, further supporting the absence of Ncb5or in the vesicles.

Our findings are not completely antagonistic to the earlier report on the ER localization of Ncb5or [15]. We clearly showed the presence of this particulate protein in the cytosolic compartment in HEK293 and HepG2 cell lines as well as in rat liver tissue, and we also demonstrated its absence within the liver microsomal vesicles. It cannot be ruled out, however, that in certain metabolic conditions, Ncb5or might be in direct physical contact with SCD1 in the ER membrane and hence loosely and/or temporarily attached to the outer surface of the ER. It seems plausible that intensified acyl-CoA desaturase activity may summon Ncb5or to reinforce the electron supply of SCD1, and this could stabilize the attachment of the protein to the ER membrane. The methodological differences (e.g., different separation of subcellular organelles or detection of another marker protein of the ER) do not explain the antithetical conclusions of the previous well-performed and correctly documented study on the subcellular localization of Ncb5or [15] and the present work. It is more likely that the cultured cells and liver tissues were analyzed in distinct metabolic states, that is, at different times after medium exchange and different periods of fasting. The potential translocation of Ncb5or between the cytosol and the ER membrane and its mechanisms deserve further investigation.

Collectively, our results contradict the channeling of ER luminal reducing equivalents into fatty acid desaturation by Ncb5or, and they strongly indicate the cytosolic localization of the protein in accordance with the lack of ER-targeting signals in the polypeptide. It remains to be elucidated, how and in which conditions Ncb5or participates in fatty acid desaturation as an alternative cytosolic electron supplier. This activity requires the protein to directly interact with integral membrane proteins of the ER. It is, therefore, likely that Ncb5or can be associated transiently to the cytosolic surface of the organelle. Further study is needed to reveal the contribution of this enzyme to the protection of pancreatic β-cells against lipotoxicity.

Acknowledgements

We thank Mrs. Valéria Mile for her skillful technical assistance. This work was supported by the Hungarian Scientific Research Fund (OTKA 104113 and 106060). Éva Kereszturi is a grantee of the János Bolyai Research Scholarship of the Hungarian Academy of Sciences.

Author contributions

EK and MC conceived and supervised the study VZ, EK and MC designed experiments VZ, EK, MT, KS, PS, FS and GL performed experiments EK, GL and MC analyzed data VZ and MC wrote the manuscript EK, MT, KS, PS, FS and GL made manuscript revisions.

References

1 Waku K (1992) Origins and fates of fatty acyl-CoA esters. *Biochim Biophys Acta* **1124**, 101–111.

2 Jakobsson A, Ericsson J and Dallner G (1990) Metabolism of fatty acids and their incorporation into phospholipids of the mitochondria and endoplasmic reticulum in isolated hepatocytes determined by isolation of fluorescence derivatives. *Biochim Biophys Acta* **1046**, 277–287.

3 Csala M, Marcolongo P, Lizak B, Senesi S, Margittai E, Fulceri R, Magyar JE, Benedetti A and Banhegyi G (2007) Transport and transporters in the endoplasmic reticulum. *Biochim Biophys Acta* **1768**, 1325–1341.

4 Jansson I and Schenkman JB (1977) Studies on three microsomal electron transfer enzyme systems. Specificity of electron flow pathways. *Arch Biochem Biophys* **178**, 89–107.

5 Miyazaki M and Ntambi JM (2003) Role of stearoyl-coenzyme A desaturase in lipid metabolism. *Prostaglandins Leukot Essent Fatty Acids* **68**, 113–121.

6 Castro LF, Wilson JM, Goncalves O, Galante-Oliveira S, Rocha E and Cunha I (2011) The evolutionary history of the stearoyl-CoA desaturase gene family in vertebrates. *BMC Evol Biol* **11**, 132.

7 Borgese N, D'Arrigo A, De Silvestris M and Pietrini G (1993) NADH-cytochrome b5 reductase and cytochrome b5 isoforms as models for the study of post-translational targeting to the endoplasmic reticulum. *FEBS Lett* **325**, 70–75.

8 Mihara K, Sato R, Sakakibara R and Wada H (1978) Reduced nicotinamide adenine dinucleotide-cytochrome b5 reductase: location of the hydrophobic, membrane-binding region at the carboxyl-terminal end and the masked amino terminus. *Biochemistry* **17**, 2829–2834.

9 Kuroda R, Kinoshita J, Honsho M, Mitoma J and Ito A (1996) *In situ* topology of cytochrome b5 in the endoplasmic reticulum membrane. *J Biochem* **120**, 828–833.

10 Oshino N, Imai Y and Sato R (1971) A function of cytochrome b5 in fatty acid desaturation by rat liver microsomes. *J Biochem* **69**, 155–167.

11 Spatz L and Strittmatter P (1973) A form of reduced nicotinamide adenine dinucleotide-cytochrome b 5 reductase containing both the catalytic site and an additional hydrophobic membrane-binding segment. *J Biol Chem* **248**, 793–799.

12 Ozols J (1976) The role of microsomal cytochrome b5 in the metabolism of ethanol, drugs and the desaturation of fatty acids. *Ann Clin Res* **8** (Suppl 17), 182–192.

13 Deng B, Parthasarathy S, Wang W, Gibney BR, Battaile KP, Lovell S, Benson DR and Zhu H (2010) Study of the individual cytochrome b5 and cytochrome b5 reductase domains of Ncb5or reveals a unique heme pocket and a possible role of the CS domain. *J Biol Chem* **285**, 30181–30191.

14 Larade K, Jiang Z, Zhang Y, Wang W, Bonner-Weir S, Zhu H and Bunn HF (2008) Loss of Ncb5or results in impaired fatty acid desaturation, lipoatrophy, and diabetes. *J Biol Chem* **283**, 29285–29291.

15 Zhu H, Larade K, Jackson TA, Xie J, Ladoux A, Acker H, Berchner-Pfannschmidt U, Fandrey J, Cross AR, Lukat-Rodgers GS *et al.* (2004) NCB5OR is a novel soluble NAD(P)H reductase localized in the endoplasmic reticulum. *J Biol Chem* **279**, 30316–30325.

16 Mandl J, Meszaros T, Banhegyi G, Hunyady L and Csala M (2009) Endoplasmic reticulum: nutrient sensor in physiology and pathology. *Trends Endocrinol Metab* **20**, 194–201.

17 Czegle I, Piccirella S, Senesi S, Csala M, Mandl J, Banhegyi G, Fulceri R and Benedetti A (2006) Cooperativity between 11beta-hydroxysteroid dehydrogenase type 1 and hexose-6-phosphate dehydrogenase is based on a common pyridine nucleotide pool in the lumen of the endoplasmic reticulum. *Mol Cell Endocrinol* **248**, 24–25.

18 Zhu H, Qiu H, Yoon HW, Huang S and Bunn HF (1999) Identification of a cytochrome b-type NAD(P)H oxidoreductase ubiquitously expressed in human cells. *Proc Natl Acad Sci USA* **96**, 14742–14747.

19 Nothwehr SF and Gordon JI (1990) Targeting of proteins into the eukaryotic secretory pathway: signal peptide structure/function relationships. *BioEssays* **12**, 479–484.

20 Pelham HR (1990) The retention signal for soluble proteins of the endoplasmic reticulum. *Trends Biochem Sci* **15**, 483–486.

21 Brown J, Novak EK, Takeuchi K, Moore K, Medda S and Swank RT (1987) Lumenal location of the microsomal beta-glucuronidase-egasyn complex. *J Cell Biol* **105**, 1571–1578.

22 Zhen L, Baumann H, Novak EK and Swank RT (1993) The signal for retention of the egasyn-glucuronidase complex within the endoplasmic reticulum. *Arch Biochem Biophys* **304**, 402–414.

23 Csala M, Banhegyi G and Benedetti A (2006) Endoplasmic reticulum: a metabolic compartment. *FEBS Lett* **580**, 2160–2165.

24 Czegle I, Csala M, Mandl J, Benedetti A, Karadi I and Banhegyi G (2012) G6PT-H6PDH-11betaHSD1 triad in

the liver and its implication in the pathomechanism of the metabolic syndrome. *World J Hepatol* **4**, 129–138.

25 Kereszturi E, Kalman FS, Kardon T, Csala M and Banhegyi G (2010) Decreased prereceptorial glucocorticoid activating capacity in starvation due to an oxidative shift of pyridine nucleotides in the endoplasmic reticulum. *FEBS Lett* **584**, 4703–4708.

26 Senesi S, Legeza B, Balazs Z, Csala M, Marcolongo P, Kereszturi E, Szelenyi P, Egger C, Fulceri R, Mandl J *et al.* (2010) Contribution of fructose-6-phosphate to glucocorticoid activation in the endoplasmic reticulum: possible implication in the metabolic syndrome. *Endocrinology* **151**, 4830–4839.

27 Szelenyi P, Revesz K, Konta L, Tutto A, Mandl J, Kereszturi E and Csala M (2013) Inhibition of microsomal cortisol production by (-)-epigallocatechin-3-gallate through a redox shift in the endoplasmic reticulum – a potential new target for treating obesity-related diseases. *BioFactors* **39**, 534–541.

28 Pierleoni A, Martelli PL, Fariselli P and Casadio R (2007) eSLDB: eukaryotic subcellular localization database. *Nucleic Acids Res* **35**, D208–D212.

29 Yu CS, Chen YC, Lu CH and Hwang JK (2006) Prediction of protein subcellular localization. *Proteins* **64**, 643–651.

30 Briesemeister S, Rahnenfuhrer J and Kohlbacher O (2010) Going from where to why – interpretable prediction of protein subcellular localization. *Bioinformatics* **26**, 1232–1238.

31 Pierleoni A, Martelli PL, Fariselli P and Casadio R (2006) BaCelLo: a balanced subcellular localization predictor. *Bioinformatics* **22**, e408–e416.

32 Chou KC and Shen HB (2010) A new method for predicting the subcellular localization of eukaryotic proteins with both single and multiple sites: Euk-mPLoc 2.0. *PLoS One* **5**, e9931.

33 Hawkins J and Boden M (2006) Detecting and sorting targeting peptides with neural networks and support vector machines. *J Bioinform Comput Biol* **4**, 1–18.